

Liquefied Petroleum Gas Desulfurization by HTBN/PAN Composite Membrane

Jian Chen, Jinxun Chen, Jiding Li, Xiaolong Han, Xia Zhan, Cuixian Chen

Department of Chemical Engineering, Tsinghua University, Beijing 100084, China

Received 27 May 2009; accepted 22 January 2010

DOI 10.1002/app.32145

Published online 13 April 2010 in Wiley InterScience (www.interscience.wiley.com).

ABSTRACT: Hydroxyl-terminated polybutadiene/acrylonitrile (HTBN) polymer material was selected for deep desulfurization of liquefied petroleum gas (LPG) according to the solubility parameter method, and then crosslinked HTBN membranes were prepared, in which asymmetric polyacrylonitrile (PAN) membranes prepared with phase inversion method acted as the microporous supporting layer in the flat-plate composite membrane. The different function compositions of composite membranes were characterized by reflection FTIR in order to investigate the crosslinking reaction. The surface and section of composite membranes were investigated by scanning electron microscope (SEM). The composite membranes prepared in this study were used in LPG for deep desulfurization. Effects of amount of HTBN and operation pressure on the desul-

furization efficiency of LPG were investigated experimentally. Experiment results demonstrated that with the membrane having a HTBN layer of 11 μm , permeability parameter of methyl mercaptan came to 17,002 Barrer and that of hydrocarbon came to 504 Barrer at 30 wt % of HTBN and 0.25 MPa, which showed that the membrane used to desulfurization in LPG can achieve high-removal efficiency. These results demonstrated that the membrane separation method could be significant in practical application for deep desulfurization of LPG. © 2010 Wiley Periodicals, Inc. *J Appl Polym Sci* 117: 2472–2479, 2010

Key words: HTBN; PAN; desulfurization; liquefied petroleum gas; membranes

INTRODUCTION

Liquefied petroleum gas (LPG) is the main household fuels in many cities all over the world, especially in China. However, sulfur present in LPG results in SO_x air pollution, which is directly responsible for acid rain. Ultra-deep removal of sulfur from transportation fuels, particularly from LPG, has become very important in petroleum refining industry worldwide. The need for cleaner burning fuels

has resulted in continuous worldwide efforts to reduce the sulfur levels in LPG. The reduction of LPG sulfur has been considered to be an important means for improving air quality.^{1–3}

A number of solutions, such as Merox process,^{4,5} have been suggested to reduce sulfur in LPG, but none of them have been proven to be ideal. Traditionally, hydrotreating process is the most effective technology used for removal of organic sulfurs present in industry. However, this technology suffers from the high investment and operating costs. It should be important to find advanced technology to remove the organic sulfur present in gasoline.

Membrane separation technology, compared with traditional separation technology, such as distillation, molecular sieve, extraction, has many advantages: (1) High separation efficiency, (2) low energy consumption, (3) simple operation, and so on.^{6,7} Kong and coworkers applied crosslinked polyethylene glycol (PEG) membranes in sulfur removal from fluid catalytic-cracking (FCC) gasoline, and the results indicated that sulfur enrichment factor came to 4.83 as flux was 0.64 $\text{kg}/\text{m}^2\text{h}$.^{8–10} In our previous work,^{11–14} polydimethylsiloxane (PDMS)/polyacrylonitrile (PAN) composite membranes were studied and applied for pervaporative desulfurization for model gasoline. However, deep desulfurization of LPG was scarcely investigated by membrane

Correspondence to: J. Li (lijiding@mail.tsinghua.edu.cn).

Contract grant sponsor: Major State Basic Research Program of China; contract grant number: 2009CB623404.

Contract grant sponsor: National Natural Science Foundation of China; contract grant numbers: 20736003, 20906056.

Contract grant sponsor: National High Technology Research and Development Program of China; contract grant numbers: 2007AA06Z317, 2008EG111021.

Contract grant sponsor: Foundation of Ministry of Education of China; contract grant number: 20070003130.

Contract grant sponsor: Foundation of the State Key Laboratory of Chemical Engineering; contract grant number: SKL-ChE-08A01.

Contract grant sponsor: Postdoctor Science Foundation of China; contract grant number: 023201069.

Journal of Applied Polymer Science, Vol. 117, 2472–2479 (2010)
© 2010 Wiley Periodicals, Inc.

technology in detail, whereas gas membrane separation was more difficult and sulfur in gas was arduous to remove.

In this study, based on solubility parameter analysis, HTBN polymer material was selected for deep desulfurization of LPG. HTBN, new membrane material, has not been extensively investigated for the separation of various mixtures.¹⁵ Moreover, microporous PAN ultrafiltration membranes were used as supporting layer of the composite membranes, whereas PAN and HTBN both have —CN bond so their interface could cement closely. Subsequently, HTBN/PAN composite membranes were prepared and used to LPG system. The influences of concentration of HTBN and operation pressure on the separation performance of the membranes were investigated experimentally in order to obtain more practical membrane preparation condition for the scale up of membrane separation technology, which is the most important point for practical application.

EXPERIMENTAL

Materials

The hydroxyl-terminated polybutadiene/acrylonitrile liquid rubber (HTBN), as shown in Figure 1, with molar mass of 2.96×10^3 , polydispersity index of 1.77 and hydroxyl group value of 0.5672 mmol/g, available from Qilong Chemical Industry Co. PAN powder was obtained from Shanghai Petrochemical Company, which contained 6% methyl methacrylate (MMA) and 0.3% 2-methyl-2-propene-1-sulfonate as co-monomers ($M_w = 75,000$). *N*-methyl pyrrolidone (NMP) was obtained from Beijing Yili Fine Chemicals Co., Beijing, China. Toluene diisocyanate (TDI), a 80/20 mixture of 2,4 and 2,6 isomers supplied by Chengdu Union Chemical Reagent Research Institute, analytically pure (AP), was purified by vacuum distillation (8.638×10^3 Pa, 148°C). Toluene and dibutyltin dilaurate (DBTL) were purchased from Tianjin Chemical Company of China for the preparation of HTBN membrane. All the chemicals used in the experiments were of analytical grade and were used without any further purification.

Membrane preparation

Supporting PAN UF membranes preparation

PAN was used as a membrane material after being dried in vacuum at 150°C for 6 h. 20 wt % of PAN was dissolved in NMP at 80°C by stirring for 12 h and then the casting solution was filtrated to get rid of impurity. To remove air bubbles, the casting solution was kept at room temperature for 24 h under vacuum. After degassing, the casting solution was cast on a polyester nonwoven fabric with a scraper

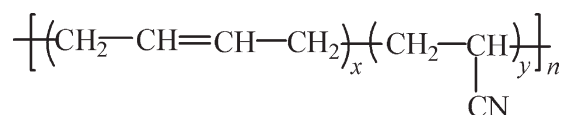


Figure 1 The chemical structure of HTBN.

of 150 μm thickness. The nascent membrane was dried for 10 s at 25°C. Then, it was immersed into DI water at 25°C. After the immersion, the precipitated membranes were washed for 12 h to remove residues of solvent mixtures from the membranes.

Composite membranes preparation

HTBN, crosslinking agent TDI, and catalyst DBTL were dissolved in toluene at room temperature. After being degassed under vacuum, the solution was cast onto the PAN membrane with a scraper of 20 μm thickness. The membrane was first vulcanized under room temperature to evaporate the solvent, and then introduced into a vacuum oven to complete crosslinking. Controlling the HTBN concentration or the coating amount could produce membranes with variable top layer thickness. The thickness of the top skin layer could be determined by means of scanning electron microscope (SEM) photographs.¹⁶ All experiments, in this study, were performed with the same membrane operation procedure.

Membrane characterization

Scanning electronic microscopy

To investigate the membrane structure, SEM characterization of the prepared membranes had been carried out. For this purpose, the membrane samples were fractured under liquid nitrogen and then coated with Au/Pd under vacuum conditions. The cross-section and surface membrane morphologies were taken by scanning electronic microscopy (JSM-7401F SEM).

Fourier transform infrared spectra—attenuated total reflection (FTIR-ATR)

Information about the presence of specific functional groups of the prepared membrane surfaces was obtained by a Nicolet IR 560 spectrometer with horizontal ATR accessory equipped with a ZnSe crystal. For evaluation, a total of 32 scans were performed at a resolution of 4 cm⁻¹ at temperature of 25°C. Meanwhile, FTIR spectra were recorded within the range of 4000–400 cm⁻¹. The software from Nicolet was used to record the spectra and for the selection of the corresponding backgrounds.

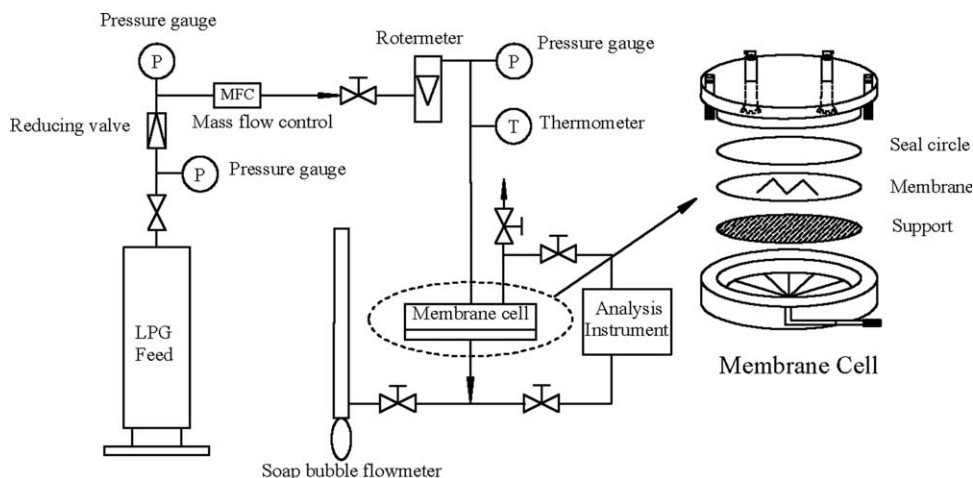


Figure 2 Scheme of the experimental apparatus.

Separation experiments

Separation experiment apparatus used in this study is shown in Figure 2. The membrane was positioned in the stainless-steel permeation cell, and the effective surface area of the membrane in contact with the feed mixture in this cell was 34.1 cm². The feed LPG was continuously circulated from a feed tank to the upstream side of the membrane in the cell at the desired temperature, and the feed temperature was monitored with a digital thermometer. After a steady state was obtained (about 1 h after start-up), mass transfer equilibrium was stable, whereas the vacuum in the downstream side of the apparatus was maintained at about 200 Pa using a vacuum pump. The compositions of the feed solution and permeation were analyzed by gas chromatography (Chengdu, WDL-94). The results were reproducible and the errors inherent in the measurements were less than 2%. The permeation flux (J) of the membrane was calculated using the expression

$$J = \frac{Q}{A \times t} \quad (1)$$

where Q (cm³, STP) is the total volume of permeation collected through the effective area of mem-

brane (A , cm²) during time (t , s) after the state has been reached.

Given that the gaseous mixture on both the feed and permeate side is ideal, the fugacity difference can be approximately equal to the partial pressure difference. The gas permeability of i component was determined by the following equation:

$$P_i = \frac{Q_i \times l}{\Delta f_i \times A} \cong \frac{Q_i \times l}{\Delta P_i \times A} \quad (2)$$

where P_i is the gas permeability of i component, Barrer (1 Barrer = 10⁻¹⁰ cm³ (STP) cm/cm² s cmHg), Q_i is the permeation flow rate of i component (cm³ (STP)/s), l is the membrane thickness (cm) determined by micrometer, Δf_i and ΔP_i are the fugacity and pressure difference of i component between feed and permeate sides (cmHg), respectively, and A is the effective membrane area (cm²).

Then the selectivity α of a membrane in a binary system is obtained as:

$$\alpha = \frac{P_A}{P_B} \quad (3)$$

TABLE I
Properties of the Main Components in the LPG¹⁸

Components	Methyl mercaptan	Propane	Propylene	Isobutane	Isobutene
Boiling point (°C)	5.9	-42.1	-47.7	-11.8	-6.8
Bond length (Å)	C-S 1.82		C=C 1.34		C=C 1.34
		C-C 1.54		C-C 1.54	
	S-H 1.33		C-C 1.54		C-C 1.54
		C-H 1.10		C-H 1.10	
Solubility parameter δ (J ^{1/2} /cm ^{3/2})	17.7	11.8	13.2	14.1	13.6
Mole fraction in LPG	400 ppm	30.8%	40.5%	14.7%	10.8%

TABLE II
Solubility Parameters of Typical Polymeric Membrane Materials

Membrane material	δ_M (J ^{1/2} /cm ^{3/2})	$\Delta\delta_A$ (J ^{1/2} /cm ^{3/2})	$\Delta\delta_B$ (J ^{1/2} /cm ^{3/2})	$\Delta\delta_A/\Delta\delta_B$
Polyacrylonitrile (PAN)	26.61	13.41	8.91	1.51
Polysulfone (PS)	21.36	8.16	3.66	2.23
Polytetrafluoroethylene (PTFE)	13.99	0.79	3.71	0.26
Polyimide (PI)	32.30	19.10	14.60	1.31
Polydimethylsiloxane (PDMS)	21.01	7.81	3.31	2.36
Polyurethane (PU)	20.98	7.78	3.28	2.37
Polyvinylpyrrolidone (PVP)	20.56	7.36	2.86	2.57
Cellulose acetate (CA)	20.06	11.86	7.36	1.61
Polystyrene (PS)	18.50	5.30	0.80	6.63
Polyvinylbutyral (PVB)	23.12	9.92	5.42	1.83
Poly(vinyl chloride) (PVC)	26.49	13.29	8.79	1.51
Poly(ethylene glycol) (PEG)	20.10	6.90	2.40	2.88
Polypropylene (PP)	21.93	8.73	4.23	2.06
Cellulose triacetate (CTA)	24.60	11.40	6.90	1.65
HTBN	17.80	4.60	0.10	46.00
Poly(vinyl acetate) (PVAC)	23.10	9.90	5.40	1.83

where P_A and P_B are the gas permeability of A and B gasses, respectively.

THEORY

Solubility parameter

Solubility parameter (δ) was proposed first by Hildebrand and Scott,¹⁷ which defined it as the square root of cohesive energy for unit volume molecule. The solubility parameter, which depends on chemical and physical structure of material, is important to characterize the interaction intensity among simple liquids and closer solubility parameter results in higher attraction for permeation components in membrane phase. The closer the solubility parameters between two substances, the better for their mutual solubility. The δ value of certain substance can be represented by its three components: Dispersion force (δ_d), polarity force (δ_p), and hydrogen bond force (δ_h). The relation is expressed as

$$\delta^2 = \delta_d^2 + \delta_p^2 + \delta_h^2 \quad (4)$$

In this study, the group contribution method for predicting solubility parameter¹⁸ was adopted and the formula was given by eq. (5):

$$\delta = \left(\frac{E_{\text{coh}}}{V} \right)^{\frac{1}{2}} = \left(\frac{\sum_i E_i}{\sum_i V_i} \right)^{\frac{1}{2}} \quad (5)$$

where E_i and V_i are internal energy and molecular volume for each structural group, respectively.

Method of membrane material selection by solubility parameter theory

Solubility parameter is effective to characterize the interaction intensity between solvent and membrane, so it is an important way for membrane materials

selection. Whether or not the membrane can fulfill its separation goal depends on the relative permeation capability of the membrane to components. The closer the solubility parameters between permeation component and membrane, the better for their mutual solubility and their separation performance. In summary, it is a feasible way to evaluate the selectivity of the membrane by estimating the interaction between polymer and solvent molecule.¹⁹

To a ternary system, including component A, component B, and membrane, the component which has closer solubility parameter with membrane should exert strong dissolution performance. That is to say, higher attraction results in the increased solubility for permeation components in the membrane. So the preferential dissolution of component A with component B in the membrane can be estimated by the

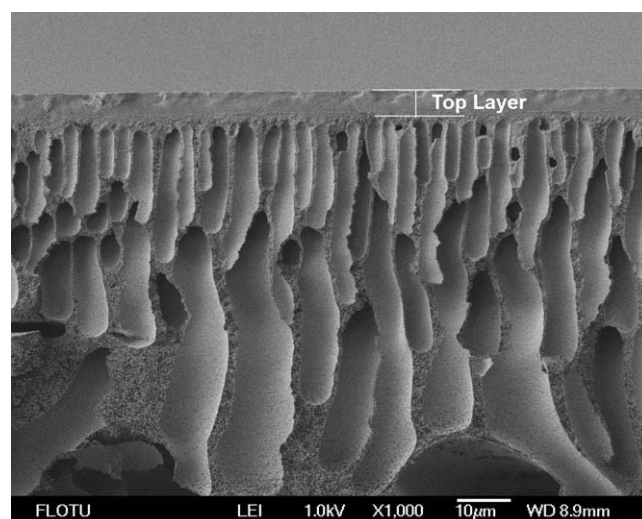


Figure 3 The cross-section morphology of the HTBN/PAN composite membrane.

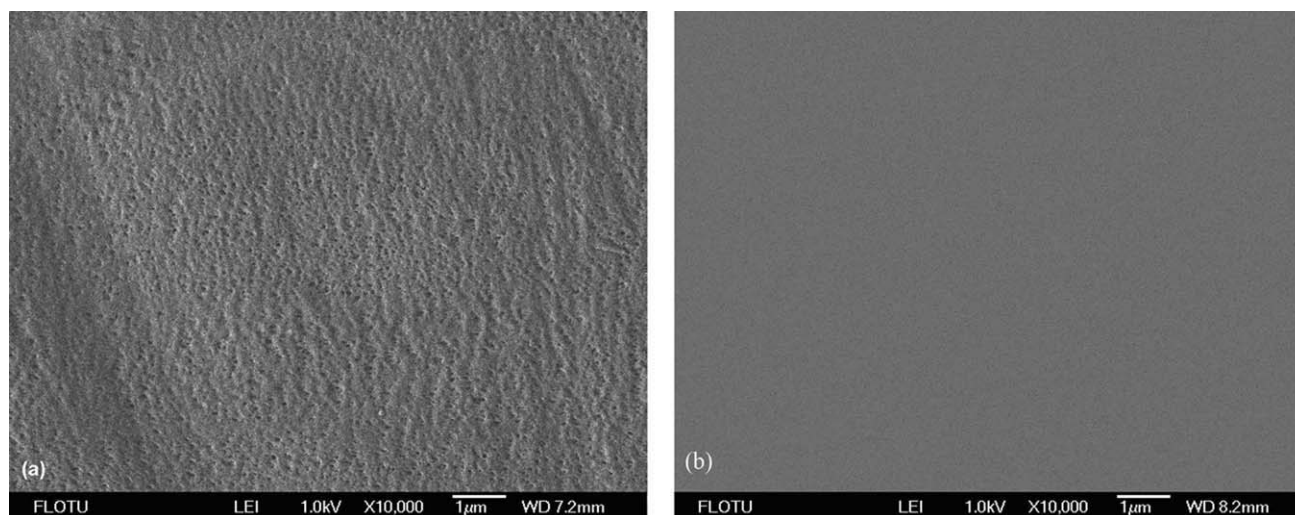


Figure 4 The surface morphology of the HTBN/PAN composite membrane.

solubility parameter theory with the quantity $\frac{\Delta\delta_A}{\Delta\delta_B}$ by eq. (6).

$$\frac{\Delta\delta_A}{\Delta\delta_B} = \frac{|\delta_A - \delta_M|}{|\delta_B - \delta_M|} \quad (6)$$

RESULTS AND DISCUSSION

Results of preliminary membrane material selection

Real LPG is a rather complex mixture composed of alkanes and olefins ranging from C3 to C5, and the main components in the LPG is propylene. Typical organic sulfur compounds in LPG is mercaptan, especially methyl mercaptan. To determine preliminary membrane material, propylene was selected to stand for LPG, whereas methyl mercaptan was chosen as the representative organic sulfur. That is, the membrane materials to be selected should permeate methyl mercaptan (component B) and prohibit propylene (component A). By calculation and query, the solubility parameters of various polymeric membrane materials were obtained, as shown in Table I.¹⁸

From Table II, the $\Delta\delta_A/\Delta\delta_B$ values of HTBN and polystyrene (PS) membrane material were far larger than that of others. Considering above analysis, HTBN and PS may have better dissolution and permeation performance to sulfur species. Furthermore, HTBN is a rubber polymer and, therefore, can offer high free volume for the diffusion of the permeate molecules. Consequently, HTBN was determined as the promising membrane material for LPG desulfurization.

SEM photographs of membranes

SEM permits imaging cross-section and surface membrane morphologies. The cross-section morphol-

ogy of the HTBN/PAN membrane was shown in Figure 3. As demonstrated in the SEM photographs, there was a clear boundary between the HTBN top layer and the PAN support layer. Meanwhile, the cross-sectional structure of the HTBN/PAN composite membrane consisted of an ultrathin-skin layer and a porous finger-like structure. Moreover, the thickness of the HTBN top layer was determined to be about 11 μm from the SEM photograph by the scale tab.¹⁶ The surface morphologies of the PAN membrane and HTBN/PAN composite membrane were shown in Figure 4(a,b), respectively. When compared Figure 4(a) with Figure 4(b), the originally porous surface of the PAN substrate was covered by a flat featureless HTBN layer, and the surface of the HTBN/PAN composite is dense and there is no pin-hole or crack. Moreover, the top composite membrane layer, functioning as the basis of selectivity, had a nonporous and tight structure, which is important for the practical application.

FTIR photographs of membranes

The attenuated total reflection Fourier transform infrared spectroscopy is a commonly used method to characterize the chemical structure of the surface.²⁰ The ATR technique enables the identification of specific molecules and groups located within 100 nm from the surface layer. To obtain detailed information about the structural changes of HTBN/PAN membranes resulting from crosslinking modification, FTIR spectra of the surface of HTBN/PAN membranes were recorded in Figure 5 using the ATR technique. From Figure 5, peaks at 2911 cm^{-1} and 2238 cm^{-1} were assigned to C–H stretching and –CN stretching, respectively. As for the strength of the –CN peak, PAN [from Fig. 5(a)] was stronger than HTBN [from Fig. 5(b)]. The reason was that

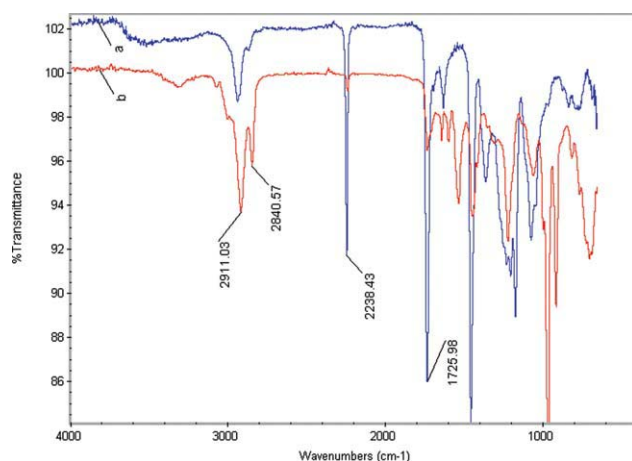


Figure 5 FTIR spectra of HTBN/PAN composite membranes: (a) PAN and (b) HTBN/PAN. [Color figure can be viewed in the online issue, which is available at www.interscience.wiley.com.]

PAN contained more $-\text{CN}$ group than HTBN and HTBN was crosslinked by $-\text{CN}$ bond, which led to the spectra of the crosslinked membranes displaying evidently weakened absorbance signals of $-\text{CN}$. These changes were the evidences of crosslinking reaction of hydroxyl-terminated HTBN with TDI under dibutyltin dilaurate catalysis. Different crosslinking agent content HTBN/PAN membranes were shown as Figure 6(a–d). From Figure 6(a–d), 3288 cm^{-1} ($\text{N}-\text{H}$ stretching) strengthened and 2238 cm^{-1} ($-\text{CN}$ stretching) weakened with the crosslinking agent content increased as more $-\text{CN}$ reacted with $-\text{OH}$ of HTBN to form a crosslinked polymer. Furthermore, 2264 cm^{-1} ($-\text{N}=\text{C}=\text{O}$ antisymmetric stretching in TDI of crosslinking agent) evidently indicated that crosslinking affected the structure of HTBN/PAN membranes because the chemical con-

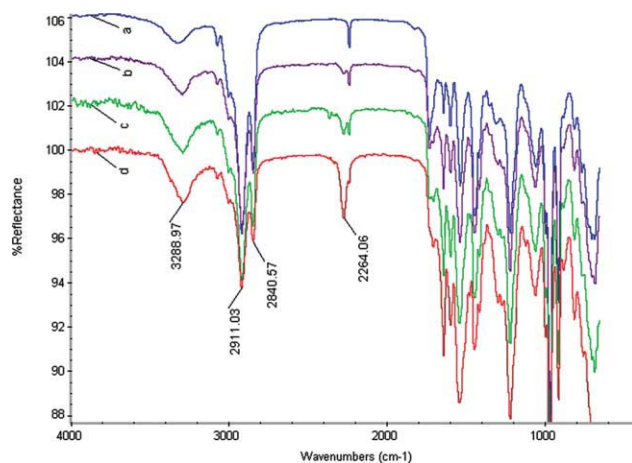


Figure 6 FTIR spectra of different crosslinking agent content HTBN/PAN membranes: (a) 2 wt %, (b) 4 wt %, (c) 6 wt %, and (d) 8 wt %. [Color figure can be viewed in the online issue, which is available at www.interscience.wiley.com.]

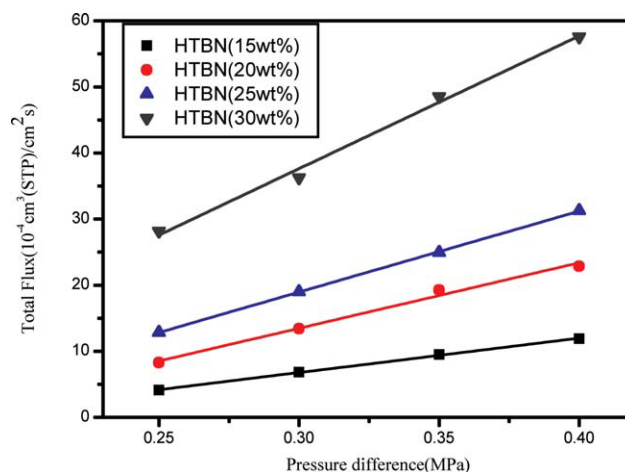


Figure 7 Effect of pressure difference on the total flux of HTBN/PAN composite membrane at 22°C . [Color figure can be viewed in the online issue, which is available at www.interscience.wiley.com.]

nection occurred between macromolecules and reticular spatial structure formed.

Effect of trans-membrane pressure (TMP) on flux

Figure 7 illustrated the effect of pressure difference on total flux at different HTBN content. In the same HTBN content, it can be observed clearly that permeation flux increased significantly with the rise of pressure difference from 0.25 to 0.4 MPa, which was consistent with common rule.²¹ Furthermore, at the same pressure difference, as shown in Figure 7, the total flux increased with the increasing of HTBN content. The separation performance is dominated by the sorption and diffusion characteristics of the individual components. This result implied that, when the HTBN content increased, more HTBN

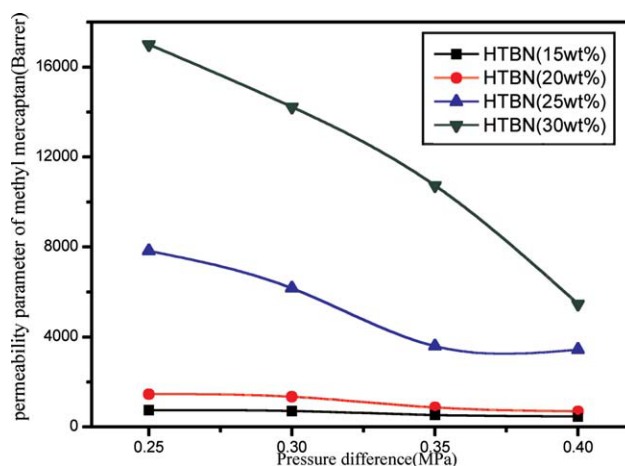


Figure 8 Effect of pressure difference on the permeability parameter of methyl mercaptan at 22°C . [Color figure can be viewed in the online issue, which is available at www.interscience.wiley.com.]

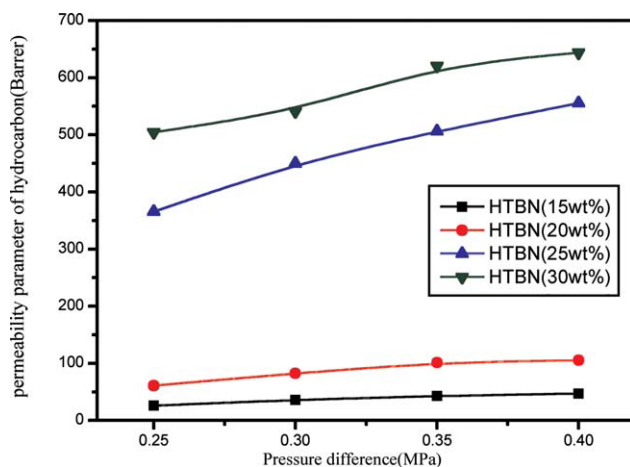


Figure 9 Effect of pressure difference on the permeability parameter of hydrocarbon at 22°C. [Color figure can be viewed in the online issue, which is available at www.interscience.wiley.com.]

chains occurred crosslinking reaction from FTIR photographs of membranes. Thereby, the top HTBN layer, functioning as the basis of permselectivity, brought out more porous network stereostructure because HTBN materials belong to rubber category. In a word, with the HTBN content increased, the free volume of HTBN membrane increased, which led to the total flux increased. In a word, the increase in total flux was due to the increase of the mobility of individual permeating molecules caused both by the pressure and by the enhanced mobility of the polymer segments.

Effect of pressure difference on permeability

The effect of pressure difference on the permeability parameter of methyl mercaptan and hydrocarbon was depicted in Figures 8 and 9, respectively. From Figures 8 and 9, it can be found that permeability of methyl mercaptan was larger than that of hydrocarbon at the same pressure difference and same HTBN content, which was attributed to the fact that methyl mercaptan permeates more easily than hydrocarbon at the same condition. It can also be explained by the data of Table II. In addition, permeability of methyl mercaptan decreased and permeability of hydrocarbon increased with pressure difference increasing at the same HTBN content. When the pressure difference increased, an extensive swelling of the membrane occurred due to the strong affinity of methyl mercaptan to the membrane. It is well-known that a remarkable swelling of polymer membranes leads to an opened membrane structure and consequently an enhancement of the permeating in the polymer membranes. Although methyl mercaptan had more privilege than other organic species to penetrate the membrane, methyl mercaptan content in LPG was

very low (ppm scale) and hydrocarbon was absolutely preponderant. Therefore, increasing pressure difference resulted in more hydrocarbons permeating in the polymer membranes, which made against methyl mercaptan permeability. In conclusion, permeability parameter of methyl mercaptan came to 17,002 Barrer and that of hydrocarbon came to 504 Barrer at 30 wt % of HTBN and 0.25 MPa, which showed that the membrane used to desulfurization in LPG can achieve high removal efficiency.

Effect of pressure difference on separation factor

From Figure 10, separation factor of methyl mercaptan decreased with the increase of pressure difference at the same HTBN content. That is to say, the permselectivity of methyl mercaptan decreased with increasing pressure gradient. In general, the permselectivity of gas separation through polymer membranes is the product of the ratio between the solubility of permeants into polymer membranes (the solubility selectivity) and the ratio between the diffusivity of permeants in polymer membranes (the diffusivity selectivity), according to the solution–diffusion theory. Thereby, the permselectivity for the LPG mixtures through the membrane depends on both solubility and diffusivity. First, the methyl mercaptan molecules that have a higher affinity for the membranes than the hydrocarbon molecules are preferentially sorbed into the membrane in the sorption process. Then, the diffusivity of these molecules in the internal membrane is significantly dependent on the molecular size and shape.¹⁴ In this case, increasing pressure difference led to a higher permeation rate and a lower separation factor as the volume of $-S-$ is bigger than that of $-C-$.

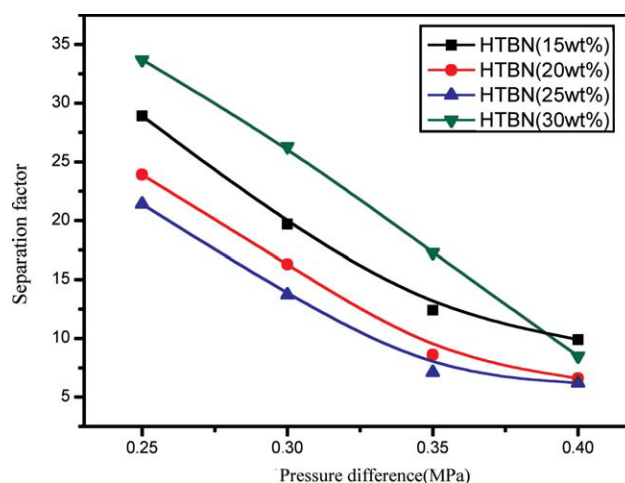


Figure 10 Effect of pressure difference on separation factor of HTBN/PAN composite membrane at 22°C. [Color figure can be viewed in the online issue, which is available at www.interscience.wiley.com.]

Especially, exorbitant addition of crosslinking agent brought about lower flux and membrane intensity decrease for solubility restricted to crosslinking agent and above results were unfavorable for practical application. For this reason, at the range of 15–25 wt % of HTBN, separation factor almost decreased with HTBN content increasing at the same pressure difference. Furthermore, separation factor had a point of transition at 30 wt % of HTBN content. That is, up to the 30 wt % of the HTBN, separation factor exerted higher level. It could be explained that the hydrocarbon penetrated very difficultly when the interchain free volume of HTBN membrane decreased at a definite degree. In conclusion, separation factor came to 33.7 at 30 wt % of HTBN and 0.25 MPa, which was more practical and efficient for the scale up of membrane technology.

CONCLUSIONS

Selection membrane material is important fundamental research for LPG desulfurization by membrane process. In this research, solubility parameters of LPG main components and typical polymeric membrane materials were calculated and given out. For methyl mercaptan, which is the primary content in sulfur species, solubility parameter was about $17.7 \text{ J}^{1/2}/\text{cm}^{3/2}$, whereas about $11\text{--}14 \text{ J}^{1/2}/\text{cm}^{3/2}$ for most other hydrocarbon species in LPG. The distinct difference in solubility parameters between them was just the key to fulfill the desulfurization. By the solubility parameter theory and membrane preparation experiments, HTBN was determined as the promising membrane material for LPG deep desulfurization.

Simultaneously, HTBN/PAN composite membranes were prepared based on the selected membrane material. The effects of the membrane preparation conditions, such as HTBN content, and the operation conditions, such as pressure difference on the gas separation properties were investigated. Experimental results indicated that permeability of methyl mercaptan was evidently higher than the permeabilities of other hydrocarbons. Permeation flux increased significantly with the rise of pressure

difference from 0.25 to 0.4 MPa, and the relationship between total flux and pressure difference was linear. In addition, permeability of methyl mercaptan decreased and permeability of hydrocarbon increased with pressure difference increasing at the same HTBN content. Separation factor of methyl mercaptan decreased with the increase of pressure difference. Therefore, HTBN/PAN membrane was proved to be an efficient alternative route for the removal of sulfur impurities out of LPG, which had the potential for becoming practical application.

References

1. Gasca, J.; Ortiz, E.; Castillo, H.; Jaimes, J. L.; González, U. *Atmos Environ* 2004, 38, 3517.
2. Luis, J. J.; Julio, S.; Uriel, G.; Emmanuel, G. *Atmos Environ* 2003, 37, 2327.
3. Chang, C. C.; Lo, J. G.; Wang, J. L. *Atmos Environ* 2001, 35, 6201.
4. Leitão, A.; Rodrigues, A. 1989, 44, 1245.
5. Leitão, A.; Rodrigues, A. *Chem Eng Sci* 1990, 45, 679.
6. Han, B.; Li, J.; Chen, C. *Desalination* 2002, 145, 187.
7. Li, J.; Chen, C.; Han, B.; Peng, Y.; Zou, J.; Jiang, W. *J Membr Sci* 2002, 203, 127.
8. Lin, L.; Wang, G.; Qu, H.; Yang, J.; Wang, Y.; Shi, D.; Kong, Y. *J Membr Sci* 2006, 280, 651.
9. Lin, L.; Kong, Y.; Wang, G.; Qu, H.; Yang, J.; Shi, D. *J Membr Sci* 2006, 285, 144.
10. Kong, Y.; Lin, L.; Yang, J.; Shi, D.; Qu, H.; Xie, K.; Li, L. *J Membr Sci* 2007, 293, 36.
11. Qi, R.; Zhao, C.; Li, J.; Wang, Y.; Zhu, S. *J Membr Sci* 2006, 269, 94.
12. Qi, R.; Wang, Y.; Li, J.; Zhao, C.; Zhu, S. *J Membr Sci* 2006, 280, 545.
13. Qi, R.; Wang, Y.; Li, J.; Zhu, S. *Sep Purif Technol* 2006, 51, 258.
14. Chen, J.; Li, J.; Qi, R.; Chen, C. *J Membr Sci* 2008, 322, 113.
15. Luo, Y.; Wang, C.; Li, Z. *Synth Met* 2007, 157, 390.
16. Conesa, A.; Gumí, T.; Palet, C. *J Membr Sci* 2007, 287, 29.
17. Hildebrand, J. H.; Scott, R. L. *The Solubility of Nonelectrolytes*, 3rd ed.; Reinhold, New York, 1950.
18. Allan, F. M. B. *CRC Handbook of Solubility Parameters and Other Cohesion Parameters*; Boca Raton, Florida, 1983.
19. Lapack, M. A.; Tou, J. C.; McGuffin, V. L.; Enke, C. G. *J Membr Sci* 1994, 86, 263.
20. Hillborg, H.; Gedde, U. W. *IEEE Trans Dielectr Electr Insul* 1999, 6, 5.
21. Rautenbach, R.; Strucka, A.; Melina, T.; Roks, M. F. M. *J Membr Sci* 1998, 146, 217.